HANDEXOS: TOWARDS A SUPPORT DEVICE FOR HAND ACTIVITIES AND TELEPRESENCE

A. Chiri [(1)], F. Giovacchini [(1)], S. Roccella [(1)], N. Vitiello [(1)], E. Cattin [(1)], F. Vecchi [(1)], M.C. Carrozza [(1)]

[(1)] ***ARTS Laboratory, Scuola Superiore Sant' Anna***
Polo Sant'Anna Valdera, Viale R. Piaggio, 34;
56025 Pontedera (PI), ITALY
carrozza@sssup.it; {a.chiri; f.giovacchini; s.roccella; n.vitiello; e.cattin; f.vecchi}@arts.sssup.it

INTRODUCTION

HANDEXOS is an exoskeleton device for supporting the human hand and performing teleoperation activities. It could be used to operate both in remote-manipulation mode and directly in microgravity environments.
In manipulation mode, crew or operators within the space ship could tele-control the end-effector of a robot in the space during the execution of extravehicular activities (EVA) by means of an advanced upper limb exoskeleton. The choice of an appropriate man-machine interface (MMI) is important to allow a correct and dexterous grasp of objects of regular and irregular shapes in the space. Many different technologies have been proposed, from conventional joysticks to exoskeletons, but the arising number of more and more dexterous space manipulators such as Robonaut [1] or Eurobot [2] leads researchers to design novel MMIs with the aim to be more capable to exploit all functional advantages offered by new space robots. From this point of view exoskeletons better suite for execution of remote control-task than conventional joysticks, facilitating commanding of three dimensional trajectories and saving time in crew's operation and training [3].
Moreover, it's important to point out that in microgravity environments the astronauts spend most time doing motor exercises, so HANDEXOS can be useful in supporting such motor practice, assisting human operators in overcoming physical limitations deriving from the fatigue in performing EVA.
It is the goal of this paper to provide a detailed description of HANDEXOS mechanical design and to present the results of the preliminary simulations derived from the implementation of the exoskeleton/human finger dynamic model for different actuation solutions.

DESIGN CRITERIA

Both the cases in which the crew is tele-controlling a dexterous space manipulator and the case in which astronauts are performing motor exercises, is extremely complicated to predict the motion required by the end-effector of the robot or by the human hand respectively. This is the reason why we decided to keep the design criteria of our hand exoskeleton as general as possible in terms of Range of Movement (RoM), degrees of freedom (DoFs) and size. An important designing goal has been the kinematic coupling between the exoskeleton and the human hand. Considering the fact that the wearable robotic system is physically coupled with the human hand, the exoskeleton design has been based on the human model in terms of biomechanics, so the centres of rotation of its axes should coincide as close as possible with the centres of rotation of the human hand. This is the most critical aspect in designing exoskeletons and it's the principal reason for which researchers often decide to reduce the number of degrees of freedom of a wearable device. Our exoskeleton, instead, allows the users full freedom of hand motion with a low level of mechanical complexity. Moreover HANDEXOS has been designed in order to provide thumb opposability; such motion is fundamental for human dexterous object manipulation, but the high level of complexity in assisting it, represents the primary cause for which in most cases hand exoskeletons do not provide thumb opposition. Another important

requirement has been the universality: usually exoskeletons are custom-made devices because of the large differences in human sizes, while HANDEXOS has been designed in order to partially fit over hands of different size through a passive and adjustable mechanism on the proximal and intermediate phalanges.

MECHANICAL DESIGN

The mechanical design of HANDEXOS has been conceived in order to achieve the following requirements: 5-fingers independent modules, an additional mechanism on the dorsum for thumb opposition (Fig. 1), natural finger movement, good wearability, comfort, low encumbrance, light weight and low inertia.

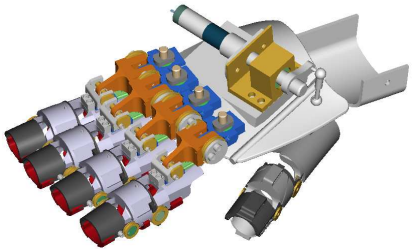

Fig. 1. Design of HANDEXOS

HANDEXOS is composed of orthotic shell structures connected by translational and rotational joints. Passive translational joints are used to ensure kinematic compatibility between human and exoskeleton's rotational axes, as well as a compliant material placed inside the shells that fits the human finger anatomy. Moreover each finger is provided with three active rotational joints. Six pulleys, two for each joint, are placed on both sides of HANDEXOS finger module in correspondence with the wearer's rotational joints. Such active joints are used for flexion/extension of Distal-Inter-Phalangeal (DIP), Proximal-Inter-Phalangeal (PIP) and Metacarpo-Phalangeal (MP) joints; moreover the MP joint has been provided with another passive rotational joint for abduction/adduction (Fig. 2-3).

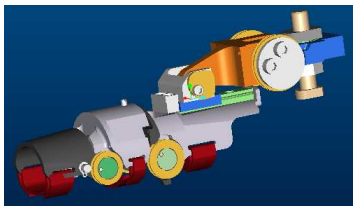

Fig. 2. Detail of a finger module

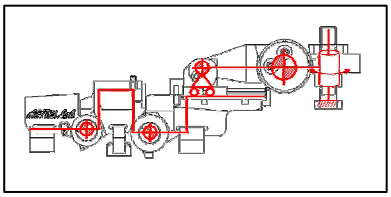

Fig. 3a. Kinematic of a finger module

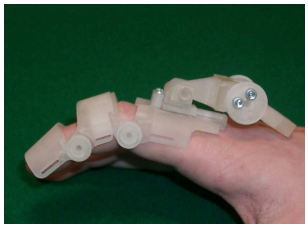

Fig. 3b. Mock-up of a finger module

The thumb module, then, has been designed in order to follow as best as possible the human thumb opposability, so a detailed analysis of its biomechanics has been necessary. The kinematic of the thumb is particularly complex because its complete motion can be described through five rotational axes: Inter Phalangeal (IP) joint has a flexion-extension axis, while the Metacarpo Phalangeal (MCP) and Carpo-Metacarpal (CMC) joints have a flexion-extension and an adduction-abduction axis. More precisely CMC joint has a third degree of freedom that is the axial prono-supination that is not independent from the flexion-extension and adduction-abduction angles but all simultaneously operate to obtain

the so called thumb opposability [5][6]. In order to simplify such kinematics, we have decided to remove MCP adduction-abduction motion, while the flexion-extension of the IP and MP joints and the opposability movement have been provided. The CMC joint motion is achieved through an additional mechanism placed on the dorsum of HANDEXOS (in order to preserve the palm area free) directly actuated by an on-board DC motor powering the thumb in order to approach the palm approximately following the human thumb opposition motion.

FINGER DYNAMIC MODEL

The dynamic model of HANDEXOS has been developed in order to be as close as possible to the biomechanics of the human hand, therefore the dynamic equations for each of the following blocks have been analyzed (see Fig. 4):

- biomechanics of human fingers and mechanics of HANDEXOS finger modules;
- mechanics of the human/exoskeleton interface;
- actuation and transmission system.

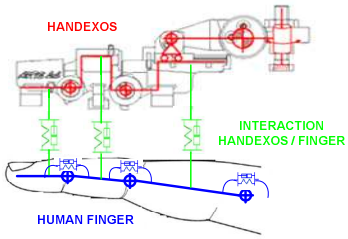

Fig. 4. Kinematic model of the HANDEXOS/human finger

The dynamic behavior of a standard human finger inside the exoskeleton finger module has been explored through the Lagrange model of a three-link planar manipulator [7]. The equations of motion of the HANDEXOS finger module coupled with the human finger (considering the friction but not the gravity effect because of the application) can be written in a compact matrix form which represents the joint-space dynamic model as:

$$B(q)\ddot{q}+C(q,\dot{q})\dot{q}-F_v\dot{q}=\tau+\tau_P \qquad (1)$$

where $q,\dot{q},\ddot{q}$ are respectively the (3x1) joint position, velocity and acceleration vectors, $B(q)$ is the (3x3) joint inertia matrix, $C(q,\dot{q})$ is the (3x3) matrix of centrifugal and Coriolis torques, F_v is the (3x3) matrix of viscous friction coefficients, τ is the (3x1) vector of the actuation torques and τ_P is the (3x1) vector of the human joints passive torques. Such passive torques are strictly related with the biomechanics of the human hand because muscles, ligaments, synovial fluid and skin tissues contribute significantly to joints stiffness and damper (as illustrated in Fig. 4) that directly influence the dynamic of the fingers resulting in a resistance to flexion movement. The expression of the passive torques is following reported:

$$\tau_{Pj} = D_j\ddot{q}_j + K_j(q_j - q_{0j}) \qquad \text{j=(1,2,3)} \qquad (2)$$

where K and D are the MCP, PIP and DIP stiffness and damping coefficients respectively for j=1,2,3 and q_0 is the mean joint angle at which the passive torque equals zero, represented by the intersection points with the horizontal line in Fig. 5. While joint damping can be described as a constant, joint stiffness exhibits a parabolic relationship with joint angle and the resultant torques as measured in [8] are following illustrated.

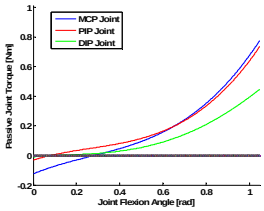

Fig. 5. Passive human joint torques

Another critical aspect to be considered is the mechanical model of the extended human/exoskeleton interaction that we have modeled exploiting a concentrated parameters model with spring-damper characteristic (see Fig. 4). Even if the skin is an heterogeneous and anisotropic material, whose mechanical properties are particularly complex, it reacts to external stress like a mono layer material with visco-elastic behavior [9]. To simplify the model of interaction, the Kelvin Voigt skin model has been exploited so that the values of the spring and dash pot do not depend on frequency. Main values for skin stiffness (Ks=87.8 N/m) and damper (Bs= 0.1005 Ns/m) have been chosen [9].

ACTUATION/TRANSMISSION SYSTEM

The modelling phase has been completed by considering the actuation system (DC motors) and the transmission system through Bowden cables. Such cable transmission choice is critical especially for its intrinsic friction losses but it is necessary in order to develop a wearable system with low inertia and a remote actuation that could be assembled on the forearm exoskeleton module or backward the astronaut. The dynamic performances of the exoskeleton are consequently strictly dependent on the adopted transmission solution.
HANDEXOS and its actuation block have been designed on purpose in order to support different actuation/transmission solutions, following listed:

- Agonist-antagonist independent-joint actuation with series non linear springs (reported as *a* in Fig. 6);
- Independent-joint actuation with series linear springs (reported as *b* in Fig. 6);
- Agonist-antagonist underactuation with non linear springs (reported as *c* in Fig. 6);
- Underactuation with linear springs (reported as *d* in Fig. 6).

Each option has its advantages and disadvantages (see Fig. 6) basically expressed in terms of required number of actuators and achievable sensory information that directly influence the number of controllable variables.

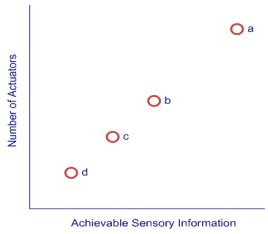

Fig. 6. Representation of advantages and disadvantages for each actuation/transmission solution

In this paper we are going to analyze the two opposite options illustrated as (a) and (d) in Fig.6 as representative of the independent-joint and underactuation categories. Each one has been tested by the HANDEXOS finger simulator implemented in LabVIEW® environment (*National Instruments LabVIEW 8.2*) and preliminary results are below shown.

Agonist-Antagonist Independent-Joint Actuation With Series-Non Linear Springs

The first proposed solution is a tendon driven agonist-antagonist system with series-non linear springs. Both extension and flexion are independent-joint actuated through a pair of cables (each one running across one of the two pulleys placed on both sides of the

exoskeleton) powering each joint independently and connected to a slider driven by a DC motor (the concept for each joint is reported in Fig. 7). This solution allows to mimic the force-elongation characteristic of the human muscle-tendon complex in order to simultaneously and independently control both single joints angles and stiffness without feedback loops [10].

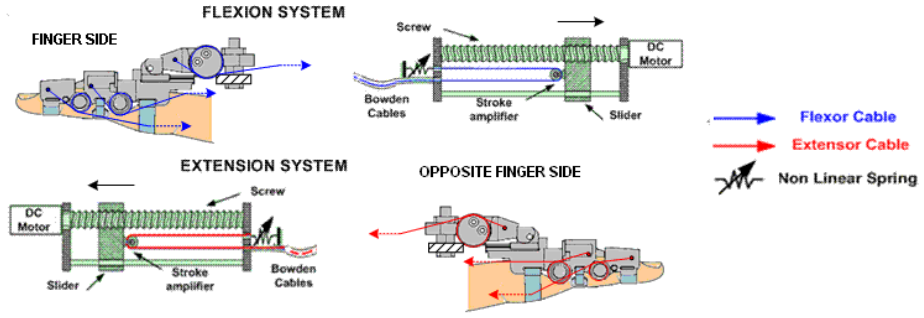

Fig. 7. Agonist-antagonist independent-joint actuation with series-non linear springs

The dynamic model of the coupled HANDEXOS/human finger modules (Fig. 4), has been implemented in MATLAB® SimMechanics and the inverse dynamic problem has been solved determining the required joints flexion torques (τ_i) resulting from the desired joints trajectories (q_i), velocities ($\dot{q}_i$) and accelerations ($\ddot{q}_i$) whose values are reported in Fig. 8 (a representative flexion time of 10 seconds has been considered), while the needed tension to allow such trajectories is illustrated in Fig. 9. In this preliminary analysis phase we have considered that the extension cable is appropriately control in order to provide no resistant torques during the flexion movement.

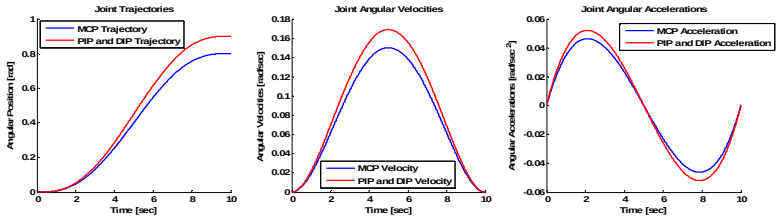

Fig. 8. Angular trajectories, velocities and accelerations at each joints

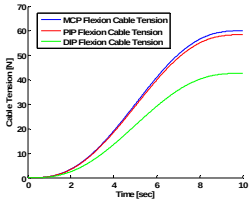

Fig. 9. Flexion tension

Such tensions are generated by each of the non linear springs placed in series with the transmission cables (see Fig. 7) whose displacement is related to the motor and joint angular position as following reported:

$$T_i = a_i\{\theta_{Mi} rr_i - [(q_i - q_{i0})R_i]\}^2 + b_i\{\theta_{Mi} rr_i - [(q_i - q_{i0})R_i]\} \quad (3)$$

where *rr* is the transmission ratio (0.6366 mm/rad), θ_{Mi} is the motor angular position, R_i is the pulley radius (whose values from the MCP to the DIP joints are: R_1=0.009 m, R_2= 0.008 m and R_3= 0.007 m), q_{i0} is the initial joint angular position, while a_i and b_i are the non linear spring coefficients whose values are such that the theoretical joint stiffness range results in the interval of 0.454-6 Nm/rad, 0.396-4 Nm/rad and 0.133-3 Nm/rad respectively for MCP, PIP and DIP, tuned by co-activating agonist-antagonist cables in parallel [10]. More in detail the desired joint position and stiffness level are obtained by displacing the two agonist-antagonist sliders of the same quantity but in opposite or same direction to

respectively regulate joint position or stiffness level. The theoretical joint stiffness is estimated by the following equation:

$$K_i = 2R_i^2(b_i + 2a_i\Delta l_i) \tag{4}$$

where Δl is the non linear spring elongation whose values, providing the above defined stiffness range, are reported in Tab. 1 together with a and b.

Tab. 1 Non linear spring parameters

	MCP Joint	PIP Joint	DIP Joint
Δl RANGE [mm]	0 – 5	0 – 4.7	0 – 3.1
a [N/mm^2]	3.44	3.02	4.67
b [N/mm]	2.80	3.09	1.36

The force-elongation curves for each couple of non linear springs are following shown and the estimated motor torques ensuring the desired trajectories are reported in Fig. 11.

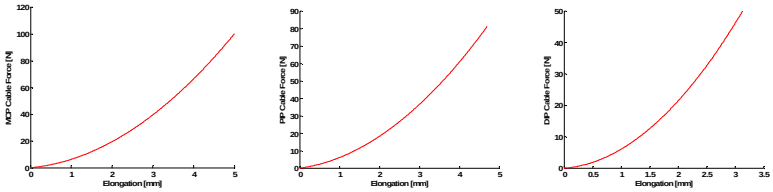

Fig. 10. Force-elongation curves of non linear springs

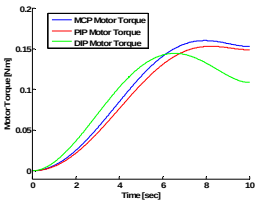

Fig. 11. Motor torques for the agonist-antagonist independent-joint solution

The great advantage coming from such actuation/transmission solution is the possibility to independently control the force on the cable, the joint angular position and the stiffness of each joint, both during the extension and flexion movement. But on the other side, the number of required actuators for each finger (six) leads to a high encumbrance and weight actuation block that represents a great drawback in designing a portable system. For this reason the most appropriate application field for the above described solution is within the space ship to tele-control the end-effector of a space-robot during EVA, exploiting the device also as an haptic interface. In fact, because of the possibility to independently control the joints stiffness, HANDEXOS could offer feedback to each joint of each finger both during extension and flexion movement in order to provide the possibility of simulating object grasping, feeling different surfaces and shapes and pushing or holding objects. In order to overpass the drawback related to the high number of actuators, a new solution is following proposed.

Underactuation With Series-Linear Springs

The new idea comes from the bio-inspired concept that is the base of our exoskeleton design. Analyzing the biomechanics of extensor and flexor finger human tendons, an underactuated solution could provide a human-like actuation allowing both the activation of all the DoFs with a natural RoM and a low encumbrance and light weight request. In fact in this case only one DC motor is used to extend DIP, PIP and MP joints and each finger is actuated by a cable running across idle pulleys, placed in each joint, and fixed to the distal phalange. The flexion of the finger is instead passively obtained by means of a set of three (one for each joint) antagonist cables running across the pulleys placed on the other side of the finger, each one connected to a remote linear spring whose elastic torque cause each

joint to flex (Fig. 12). In this case, because of the lack of an agonist-antagonist cables configuration, it is possible to only control the angular position of the three joints without any control of the finger's stiffness.

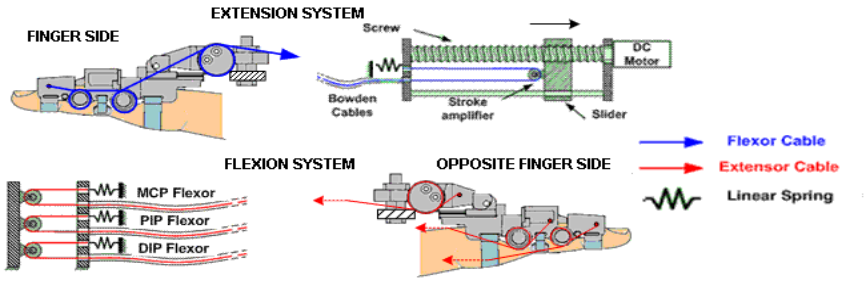

Fig.12. Underactuation with linear springs

In order to develop the dynamic model of the underactuated exoskeleton finger it has been necessary to test several simulation trials with different mechanical parameters in order to iteratively define an accurate set of pulleys radii and springs stiffness, finally resulted (from MCP to DIP joint) in: R_1= 0.009 m, R_2 = 0.006 m, R_3 = 0.005 m, K_1 = 9410 N/m, K_2 = 9200 N/m and K_3 = 13940 N/m. In this case, instead, the direct dynamic problem has been solved, once the actuation torques (6), the initial joints positions and the velocities are known. Furthermore another resistant effect has been added in the dynamic equation reported in (1) that is the effect of three forces (in this preliminary step considered constant), applied at the centre of mass of each phalange, representing the maximal resistance forces exerted by the finger of the astronaut during motor exercises with preliminary values (from the proximal to the distal phalange) of F_1=10 N, F_2=6 N, F_3=3N.
Because of the underactuation solution, the joints torques are coupled each other by the same tension T through the following relations:

$$\tau_1 = \frac{r_1 T (l_1 \cos(\Theta_1) - h \sin(q_1))}{l_1 \cos(q_1)\cos(q_1 - \Theta_1)}$$
$$\tau_2 = r_2 T$$
$$\tau_3 = r_3 T$$
$$\Theta_1 = q_1 + \frac{\arcsin(-d\cos(q_1) - h)}{l_1} \qquad (6)$$

where Θ_1 (derived from geometrical considerations), l_1 (0.029 m), h (0.0124 m) and d (0.0139 m) are reported in Fig. 13.
From the static equilibrium at the distal phalange for rest and final configurations, the initial and final values of the cable tension have been derived and its variation respect the time has been assumed to be of the fifth order; its values, the deriving three joint trajectories (see q_1, q_2 and q_3 in Fig. 13) and the estimated motor torque are following illustrated.

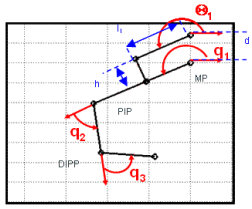

Fig. 13. Finger scheme

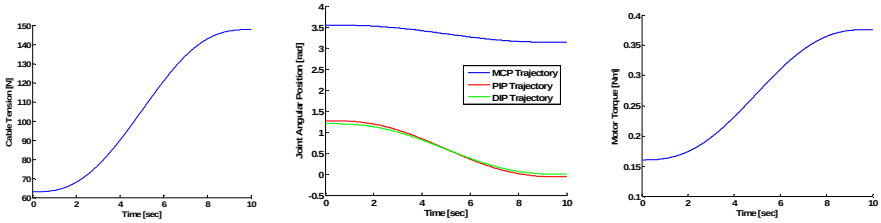

Fig. 14. Cable tension, joints trajectories and motor torque

In this configuration one only actuator is necessary to extend the finger but, as a consequence of the underactuation choice, there is no possibility to independently control each joint angular position and cable force (because of the relation reported in (6)). Furthermore there is no possibility to control the joint stiffness, however a desired stiffness level can be set at each joint at the beginning of the motion through a right pre-load of each linear spring, but without possibility to control it during the execution of different tasks. In spite of that, because of its low mass and high level of portability, the device can be very useful in assisting astronauts in performing motor practice, exercising different type of grasp and strengthening their hands.

CONCLUSION

This paper presented a powered exoskeleton hand, designed in order to try to address the requirements coming from the spatial application field. The work specifically focused on the mechanical design purpose-made in order to support different actuation/transmission systems from the most general independent-joint actuation with in series non-linear springs, to a highly bio-inspired underactuation. Moreover preliminary simulation analysis have been carried out in order to both iteratively optimize the mechanical design and to test different actuation solutions with the final aim to choose the most appropriate for supporting the human hand or performing teleoperation activities. Preliminary results show a not remarkable difference in terms of resultant RoM for each analyzed actuation/transmission system, but the number of actuators, the achievable sensory information and the kind of control strictly depend on each proposed option. Starting from this preliminary study, the future work will be oriented in a detailed experimental validation with the first HANDEXOS prototype (under fabrication) and in testing scenarios of motor exercise and teleoperation.

REFERENCES

[1] P. Schoonejans, R. Stott, F. Didot, A. Allegra, E. Pensavalle, C. Heemskerk, "Eurobot: EVA-assistant robot for ISS, Moon and Mars", *Proc. 8th ESA Workshop on Advanced Space Technologies for Robotics and Automation*, Noordwijk, November 2004.

[2] W. Bluethmann, R. Ambrose, M. Diftler, S. Askew, E. Huber, et al, "Robonaut – A robot designed to work with humans in space", *Autonomous Robots*, vol. 14, pp. 179-197, 2003.

[3] A. Schiele, M. De Bartolomei, F. van der Helm, "Towards intuitive control of space robot: a ground development facility with exoskeleton", *IEEE/RSJ Int. Conf. on Intelligent Robots and Systems*, October 2006, Beijing, China.

[4] B. L. Shields, J. A. Main, S. W. Peterson, A. M. Strauss, "An anthropomorphic hand exoskeleton to prevent fatigue during extravehicular activities", *IEEE Trans. On Systems, Man and Cybernetics*, vol. 27, no. 5, September 1997.

[5] I.A. Kapandji, "Fisiologia Articolare".

[6] L. Y. Chang, Y. Matsuoka, "A Kinematic Thumb Model for the ACT Hand", *Proc. of the 2006 IEEE International Conference on Robotics and Automation*, Florida, 2006.

[7] L. Sciavicco, B. Siciliano, "Modeling and control of robot manipulator".

[8] D. G. Kamper, W. Z. Rymer, "A Biomechanical Simulation of the Effect of the Extrinsic Flexor Muscles of Finger Joint Flexion", *Proc. 23rd Annual Conference IEEE EMBS*, Oct. 25-28, 2001, Istanbul.

[9] G. Boyer, H. Zahouani, A. Le Bot, L. Laquieze, "In vivo characterization of a viscoelastic properties of human skin using dynamic micro-indentation", *Proc. 29th Annual International Conference IEEE EMBS*, 23-26 August, 2007, Lyon.

[10] N. Vitiello, T. Lenzi, J. McIntyre, S. Roccella, E. Cattin, F. Vecchi, M. C. Carrozza, "Characterization of the NEURARM bio-inspired joint position and stiffness open loop controller", *2nd IEEE/RAS-EMBS International Conference on Biomedical Robotics and Biomechatronics*, October 19-22, 2008, Arizona.